

## Penetration of electronic perturbations of dilute nitrogen impurities deep into the conduction band of $\text{GaP}_{1-x}\text{N}_x$

S. V. Dudiy, P. R. C. Kent, and Alex Zunger

National Renewable Energy Laboratory, Golden, Colorado 80401, USA

(Received 13 July 2004; published 14 October 2004)

The electronic structure consequences of the perturbations caused by dilute nitrogen impurities in GaP are studied by means of supercell calculations using a fully atomistic empirical pseudopotential method. We find that numerous localized states are introduced by a single N atom and N clusters, not only close to the band edge but also throughout the GaP conduction band, up to  $\sim 1$  eV above the conduction band edge. These localized states suggest an alternative interpretation for a previously puzzling observation of splitting of photoluminescence excitation intensity at the GaP  $\Gamma_{1c}$  energy into two features, one blueshifting and the other staying pinned in energy with increasing N concentration.

DOI: 10.1103/PhysRevB.70.161304

PACS number(s): 71.55.Eq, 71.70.-d

Significant efforts have recently been made to understand the nature of the perturbations induced by nitrogen alloying of GaP, as observed by photoluminescence<sup>1-6</sup> (PL), its excitation<sup>7-9</sup> (PLE), ballistic electron emission,<sup>10</sup> resonant Raman scattering,<sup>11</sup> and ellipsometry<sup>12,13</sup> spectra. While initial efforts have focused on the spectral region near the indirect,  $X_{1c}$  absorption/emission threshold (2.35 eV), more recent studies<sup>7-9,13</sup> have revealed significant spectral changes not only at such low energies (LE) but also at high energies (HE), up to and exceeding the direct gap threshold  $\Gamma_{1c}$  at 2.85 eV. For example, a splitting of PLE intensity at the GaP  $\Gamma_{1c}$  energy into two features, one being blueshifted<sup>12</sup> and the other being *pinned*,<sup>7</sup> has been observed with increasing N concentration. The existence of both LE and HE nitrogen-induced perturbations already at very low concentrations,  $x \lesssim 0.5\%$ , raises the question of the nature of the coupling<sup>3,4,14,15</sup> between nitrogen impurity states and the host crystal states: Viewing the effect of nitrogen as an “impurity band”<sup>3,14</sup> (IB) formed by N impurity levels initially located below the host conduction band minimum (CBM), and gradually broadening with increased nitrogen concentration until this band touches the host CBM addresses, by construction, only the LE spectral region. Yet, profound spectral changes were seen at high energies even for low N concentration,<sup>7-9,13</sup> which remain unexplained by such a model. The clear evidence that application of pressure,<sup>16</sup> which raises the conduction band minimum, exposes *narrow* impurity levels, rules out the IB model. Furthermore, the observation<sup>17,18</sup> of an *increase* of the electron effective mass with N concentration for  $\text{GaAs}_{1-x}\text{N}_x$ , even after the alleged merging with the conduction band, also contrasts with expectations<sup>19</sup> of the IB model. The “band anticrossing” (BAC) model<sup>4</sup> views the effect of nitrogen as a coupling between a single impurity state  $a_1(N)$ , initially in the gap, with the host conduction band states. The model assumes that there is *only one* N state (the one in the GaP gap), and it predicts that both the N state and the host conduction states shift with composition. Yet, spectroscopic evidence shows *multiple* N-related peaks both at LE and HE, some of which being *pinned in energy* as the composition changes. Furthermore, the BAC model does not account for the observed

cluster states, which control the emission spectra and transport.<sup>1-3,5,6</sup> Finally, neither BAC nor IB can explain the recently observed splitting of PLE intensity at  $\Gamma_{1c}$  energy into two spectral features,<sup>7,12</sup> with one of them being blueshifted and the other being pinned as N concentration increases. It is becoming evident that simple models<sup>3,4,14</sup> do not account for the main spectroscopic features of this system.

We have taken a different approach:<sup>15,20,21</sup> instead of postulating *a priori* an energy-level model,<sup>3,4,14</sup> we first solve quantum mechanically for the detailed electronic structure, using a fully atomistic approach and permitting isolated nitrogen as well as various nitrogen clusters to interact and perturb all host states over a broad energy range. We then distill *a posteriori* from the numerical results a simple energy level model. We find multiple spectral changes not only at the LE region, but also at the HE region. Many of these ensuing states have no counterpart in any of the previous IB or BAC models. We find new localized states introduced by single N and N clusters throughout the GaP conduction band. These states suggest a new interpretation for a previously puzzling observation<sup>7,12</sup> of the split  $\Gamma_{1c}$ . We also point at the existence of *L* character just below the valence band maximum, and the coexistence of dominant cluster states at the conduction band edge.

We model the substitutional  $\text{GaP}_{1-x}\text{N}_x$  alloy systems within a supercell approach, using a large cubic  $6 \times 6 \times 6$  (1728 atom) supercell. To simulate *isolated* N we place a single N atom in it ( $x=0.12\%$ ), whereas to simulate *isolated pairs* we add one more N atom at different neighbor positions with respect to the first N atom, creating first-neighbor pairs (NN1), second-neighbor pairs (NN2), etc., up to the fourth-neighbor (NN4) position. Finally, to study diluted *alloys* we take 6, 11, and 30 nitrogen atoms and distribute them randomly over the anion sites of the same 1728 atom cell, considering 12 different randomly generated atomic realizations for each N concentration  $x$ . This simulates random alloys with  $x$  equal to 0.69%, 1.27%, and 3.51%. In all cases the electronic structures of these  $\text{GaP}_{1-x}\text{N}_x$  alloy models are calculated fully atomistically by means of the empirical pseudopotential method,<sup>15,20,21</sup> using the same computational

parameters as in Ref. 15. The atomic site positions are fully relaxed with the valence force field method (VFF)<sup>22</sup> with VFF parameters from Ref. 20. As shown in Ref. 15, VFF reproduces to within 1% the first-principles local-density approximation (LDA) calculated atomic positions and bond lengths in  $\text{GaP}_{1-x}\text{N}_x$  alloy. The pseudopotential is made of a superposition of screened atomic pseudopotentials of Ga, P, and N situated on the corresponding atomic sites. The screened atomic potentials are empirically adjusted to closely reproduce the bulk band structures, effective masses, and deformation potentials, and they include explicitly local environment<sup>23</sup> and local strain<sup>24</sup> dependencies. The electronic Hamiltonian is diagonalized in a plane-wave basis set via the folded spectrum method.<sup>25</sup> The calculated electronic states are analyzed by evaluating their  $\Gamma$ ,  $L$ , and  $X$  character using the “majority representation” projections.<sup>26</sup> Those projections are calculated by expanding the explicit wave function of a given electronic state in a complete set of Bloch wave functions and then calculating the sum over bands of the projections at a given bulk wave vector (e.g.,  $\Gamma$ ,  $L$ , or  $X$ ). The  $\Gamma$  character of a conduction band state determines the dipole matrix element squared for optical transitions to that state from the  $\Gamma$ -like  $\text{GaP}_{1-x}\text{N}_x$  valence band maximum (VBM), and is particularly relevant in PL/PLE data interpretations.

*Single nitrogen and nitrogen pairs.* Previous IB (Refs. 3 and 14) and BAC (Ref. 4) models assumed that the sole fingerprint of an isolated nitrogen impurity is the appearance of a N-localized electronic state  $a_1(\text{N})$  below the GaP conduction band. To check this assumption, Fig. 1 considers, over a broad energy range, the percentage of  $\Gamma$ ,  $L$ , and  $X$  character for the electronic states of GaP with a *single* N atom [Fig. 1(a)] or a *single* N-N pair at different separation [Fig. 1(b)–1(e)]. The hostlike states [“perturbed host states” (PHS), solid lines in Fig 1] and cluster states (CS, symbols in Fig. 1) are identified on the basis of their wave functions, as discussed above and in Ref. 15. Considering first the PHS induced by a single nitrogen [Fig. 1(a)], we see that the threefold-degenerate  $X_{1c}$  valley of pure GaP is split<sup>27</sup> into two PHS [ $a_1(X_{1c})+e(X_{1c})$ ], the fourfold  $L_{1c}$  valley is split into two PHS [ $a_1(L_{1c})+t_2(L_{1c})$ ], the threefold  $X_{3c}$  valley remains degenerate [ $t_2(X_{3c})$ ], as does the onefold  $\Gamma_{1c}$  [giving rise to  $a_1(\Gamma_{1c})$ ]. When a single N atom is introduced, these PHS shift only very little relative to their positions in pure GaP.

The most important aspect of Fig. 1 is that in contrast to the previous assumption, our calculations show that the perturbations caused by a single nitrogen atom or by a single nitrogen pair extend deep into conduction band, up to  $\sim 1$  eV above the CBM. In particular, Fig. 1 shows that there is a multitude of new states with significant  $X$ ,  $L$ , and  $\Gamma$  character (isolated symbols in Fig. 1) appearing throughout the conduction band, including the vicinity of the high-energy  $\Gamma_{1c}$  critical point. Such multiple new states appear even for a single N atom [Fig. 1(a)]. These new cluster states, except those that are near  $\Gamma_{1c}$ , have mostly  $L$  and  $X$  character, so they may not be observed in the PL or PLE data, at least for transitions from a  $\Gamma$ -like VBM. These calculated CS are used in our basic model [Fig. 3(d)] of the electronic structure of N in GaP.

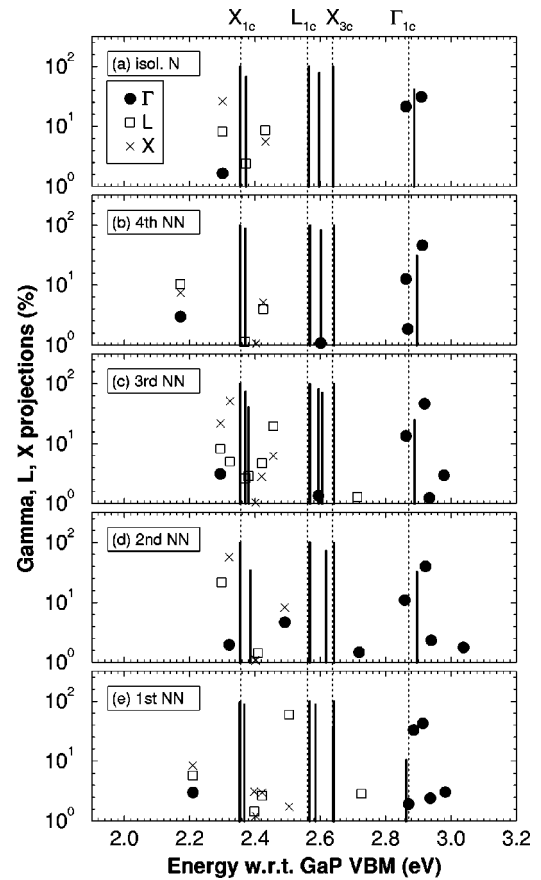


FIG. 1. Calculated energies and character of electronic states for a large (1728 atom) cubic supercell containing (a) a single N atom and (b)–(e) N pairs separated by fourth to first nearest-neighbor distances, respectively. The dotted lines show energy positions of the unperturbed GaP host states. The energies are with respect to the GaP valence band maximum of unstrained GaP. The solid vertical lines show the energy positions of the perturbed GaP host states, with the height of those lines being the  $X$ ,  $L$ ,  $X$ , and  $\Gamma$  character (in percent) for the  $X_{1c}$ ,  $L_{1c}$ ,  $X_{3c}$ , and  $\Gamma_{1c}$  perturbed host states, respectively. The isolated symbols denote N localized states (cluster states), showing their  $\Gamma$ ,  $L$ , and  $X$  character.

*Dilute alloys:* Figure 1 shows that the character and the energy positions of the newly found cluster states are quite sensitive to the specific atomic configurations (NN1 versus NN2, etc.) of the clusters. This means that in a random alloy, which, for statistical reasons, contains a variety of nitrogen environments, many cluster states from different atomic configurations are likely to be present, especially in the energy vicinity of  $X_{1c}$  and  $\Gamma_{1c}$  critical points. To examine this, we analyze the  $\Gamma$ ,  $L$ , and  $X$  character distribution for *random*  $\text{GaP}_{1-x}\text{N}_x$  alloys at finite nitrogen concentrations (Fig. 2). This allows us to see how the localized states of isolated N or isolated N-N pairs evolve and penetrate deep into the alloy conduction band. We can also make a direct comparison with the measured PLE intensity data, assuming  $\Gamma$ - $\Gamma$  transitions from the  $\text{GaP}_{1-x}\text{N}_x$  VBM, which is essentially of  $\Gamma$  character.<sup>8</sup> We have then used the results of such detailed supercell calculations to distill a simple energy-level model presented in Fig. 3. It shows how the  $X_{1c}$ ,  $L_{1c}$ ,  $X_{3c}$ , and  $\Gamma_{1c}$  band-edge states of pure GaP [Fig. 3(a)] produce perturbed

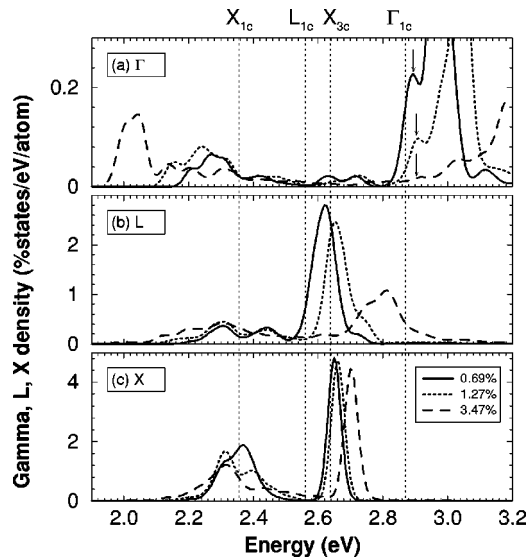


FIG. 2. Energy distribution of the (a)  $\Gamma$ , (b)  $L$ , and (c)  $X$  character densities for the  $\text{GaP}_{1-x}\text{N}_x$  alloy conduction states at different N concentration: 0.69% (solid line), 1.27% (dotted line), and 3.47% (dashed line). Each density is averaged over 12 different random atomic configurations, using a 0.02 eV Gaussian smearing. Vertical dotted lines denote the energy positions of the critical points of the pure unstrained GaP. The energies are with respect to the unperturbed GaP valence band maximum. The  $\Gamma/L/X$  densities are in units of the number of states weighted by percentage of their  $\Gamma/L/X$  character per eV per supercell atomic site (Ga,P,N). Arrows in (a) point at a pinned peak at 2.90 eV.

host states in Fig. 3(b) [viz., Fig. 1(a)], and identifies the main cluster states due to *isolated* nitrogens as well as *isolated* nitrogen pairs [viz., Figs. 1(b)–1(e) and 3(d)]. The levels of  $\text{GaP}_{1-x}\text{N}_x$  are described as a mixture of PHS and CS [Fig. 3(c)].

We divide our discussion into three energy regimes: (i) low-energy states, i.e., near and below the host  $X_{1c}$  CBM; (ii) intermediate-energy states, between  $X_{1c}$  and  $\Gamma_{1c}$ ; and (iii) high-energy states, in the vicinity of the direct band edge  $\Gamma_{1c}$ .

(i) *Low-energy states (up to  $X_{1c}$ ).* (a)  $\Gamma$  character. Figure 2(a) shows that at LE we have alloy states with strong  $\Gamma$  character. This  $\Gamma$  mixing leads to a *positive* conduction band edge pressure coefficient,<sup>4</sup> even though in pure GaP with its  $X_{1c}$ -like band edge the pressure coefficient is negative. We see that these LE states red-shift, broaden, and *increase* their intensity as the nitrogen concentration increases. Furthermore, the  $\Gamma$ -like alloy LE peak [Fig. 2(a)] exhibits clear spectral structure, due to amalgamation of cluster states being overtaken by the down shifting conduction band edge.<sup>15</sup>

(b) *non- $\Gamma$ -character.* The intensity of the  $L$  and  $X$  character [Fig. 2(b) and 2(c)] in this LE region is much stronger than that of the  $\Gamma$  character there, similar to the LE cluster states in Fig. 1. This behavior can be understood (Fig. 3) by attributing the broadening and buildup (with increasing N concentration) of the  $L$  and  $X$  intensity in this region to the growing number of cluster states, which dominate the LE region. These cluster states hybridize with LE PHS, especially with the  $a_1$  one, which is redshifted due to repulsion from the higher energy  $a_1$  PHS.<sup>15</sup> The stationary peak at  $X_{1c}$  energy observed in the resonant Raman scattering

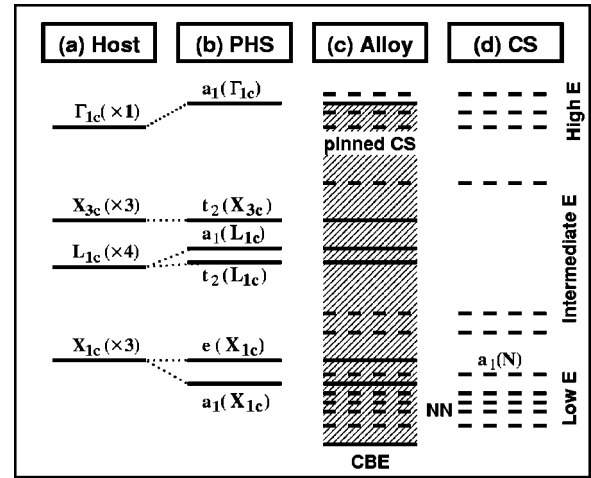


FIG. 3. Schematic energy diagram showing how the N perturbation shifts and perturbs GaP host state energy levels (a) to produce the perturbed host states (PHS) (b), as well as introduces N cluster states (CS) (d) throughout the GaP conduction band, which combines with PHS in the resulting picture of GaPN alloy states (c).

spectroscopy<sup>11</sup> is likely to come from the  $e(X_{1c})$  PHS. The cluster states couple very weakly to the  $e(X_{1c})$ , but strongly to the  $a_1$  PHS. The most clear indication of this behavior in our calculated results can be found in the  $X$  intensity curve for 0.69% N concentration in Fig. 2(c), where there is a pronounced peak at GaP  $X_{1c}$  energy, even though the conduction band edge has moved  $\sim 0.2$  eV below that energy. While at higher N concentrations there is still high  $X$  character intensity at  $X_{1c}$  energy, the  $e(X_{1c})$  PHS contribution is not clearly distinguishable. The LE edge is *not* the  $L_{1c}$  state that has plunged down, surpassing  $X_{1c}$ , as an incorrect interpretation of our Ref. 15 by the authors of Ref. 14 suggests. Note further that the rapid downward shift of the conduction band edge is caused primarily by the coupling of the CS with the *nearby*  $X_{1c}$ -derived PHS, and to a lesser extent with the remote  $\Gamma_{1c}$ -derived PHS, as suggested by the BAC model.<sup>4</sup> In contrast with the IB model, the LE states manifest a *co-existence* of pinned CS with the broad PHS.

(ii) *Intermediate-energy states (between  $X_{1c}$  and  $\Gamma_{1c}$ ).* A misunderstanding of our previous theoretical results<sup>15</sup> led to the conclusion<sup>14</sup> that due to N doping the perturbed  $L_{1c}$  point should gain some noticeable  $\Gamma$  character and move down to the conduction band edge. Unlike Ref. 14, we note, however, that the theoretical method used previously in Ref. 15 and here does not result in any noticeable  $\Gamma$ - $\Gamma$  optical transition intensity around the  $L_{1c}$  critical point, and there are no downward moving features in the  $\Gamma$  character between the 2.4 and 2.8 eV. Regarding  $\Gamma$ - $\Gamma$  transitions, in fact, Fig. 2(a) shows a practically flat plateau of  $\Gamma$  intensity in the 2.4–2.8 eV region. If we consider only conduction band states as Fig. 2 does, there is no buildup of spectral intensity in this region, and the calculated intensity (height) of this plateau of  $\Gamma$ - $\Gamma$  transitions is rather low. Yet the ellipsometry results of Kanaya *et al.*<sup>13</sup> do show significant amplitude in the  $X_{1c}$ - $\Gamma_{1c}$  region, as do the PLE results.<sup>7–9</sup> We find<sup>8</sup> a significant contribution to the amplitude (dipole transition matrix element squared) at transition energies between 2.4 and 3.0 eV, which comes from the  $L$ - $L$  like optical transitions



from the states *just below* the VBM. The growing intensity of those transitions with increasing  $x$  is due to the N induced buildup of the  $L$  character near the conduction band edge [Fig. 3(b)] and just below the VBM, down to 0.6 eV below the VBM (but still above the host  $L_{1v}$  energy). This feature cannot be accounted for by either the BAC or IB models.

We see that the main peak of  $L$  character near  $L_{1c}$  [Fig. 2(b)] and, to a lesser extent, the  $X$  peak near  $X_{3c}$  [Fig. 2(c)] blueshift with increasing nitrogen concentration. The trend for the  $L$  peak is consistent with a noticeable blueshift and decreasing intensity peak height of the  $E_1$  ( $L$ - $L$ ) transitions with increasing N concentration observed in the ellipsometry data.<sup>12,13</sup>

(iii) *High-energy states (at or above  $\Gamma_{1c}$ )*. At higher energies ( $>2.8$  eV), we find that the absorption edge at the  $\Gamma_{1c}$  critical point of GaP broadens and blueshifts due to repulsion from lower-energy  $a_1$  states (Fig. 3). The  $\Gamma$  intensity near  $\Gamma_{1c}$  also has features that shed light on the recent puzzling observation of Buyanova *et al.*<sup>7</sup> of splitting of the HE PLE intensity into two peaks, one blueshifting and the other staying *pinned* at 2.87 eV. We indeed identify a peak that is pinned in energy at 2.90 eV [in Fig. 2(a)]. This calculated peak becomes less intense with increasing nitrogen concentration, as observed experimentally.<sup>7</sup> This new energy-pinned peak does not correspond to the  $t_2(L_{1c})$  or  $t_2(X_{3c})$  states, as was thought initially,<sup>7</sup> because we find that  $X$  and  $L$  intensity peaks are located at noticeably lower energies than  $\Gamma_{1c}$ , and there are no  $L$  or  $X$  intensity features that would be pinned

near  $\Gamma_{1c}$ . Based on examination of our calculated wave functions of alloy electronic states near 2.90 eV, we identify the pinned peak at 2.90 eV as localized cluster states of single nitrogen atoms. Such isolated or semi-isolated nitrogens occur when, for statistical reasons, one N atom appears to be farther apart from other N atoms nearby. This also explains why this peak practically disappears at high enough N concentrations, both in PLE data and in our results, since at higher N concentrations there is a lower probability for a N atom to be sufficiently far from all other N atoms.

In conclusion, as summarized in Fig. 3, we find that even a single N atom introduces multiple N-localized states throughout the GaP conduction band and we identify the energy shifts of different GaP perturbed host states. Unlike the existing BAC and IB models, our polymorphous model of  $\text{GaP}_{1-x}\text{N}_x$  system, which naturally incorporates both the cluster states and perturbed host states in a single picture, allows us to capture and interpret all the key features of the measured PLE and ellipsometry data, including energies deep in the  $\text{GaP}_{1-x}\text{N}_x$  conduction band. The high energy N-localized states are essential for understanding of the PLE observed splitting of the  $\Gamma_{1c}$  absorption edge into two peaks, one pinned and the other blueshifted.

This work is supported by the U.S. Department of Energy, SC-BES-DMS Grant No. DEAC36-98-GO10337. We thank M. Capizzi and A. Polimeni for fruitful discussions.

- 
- <sup>1</sup>J. N. Baillargeon, K. Y. Cheng, G. E. Hofler, P. J. Pearah, and C. Hsieh, *Appl. Phys. Lett.* **60**, 2540 (1992).
- <sup>2</sup>S. Miyoshi, H. Yaguchi, K. Onabe, R. Ito, and Y. Shiraki, *Appl. Phys. Lett.* **63**, 3506 (1993).
- <sup>3</sup>Y. Zhang, B. Fluegel, A. Mascarenhas, H. P. Xin, and C. W. Tu, *Phys. Rev. B* **62**, 4493 (2000).
- <sup>4</sup>J. Wu, W. Walukiewicz, K. M. Yu, J. W. Ager III, E. E. Haller, Y. G. Hong, H. P. Xin, and C. W. Tu, *Phys. Rev. B* **65**, 241303 (2002); W. Shan, W. Walukiewicz, K. M. Yu, J. Wu, J. W. Ager III, E. E. Haller, H. P. Xin, and C. W. Tu, *Appl. Phys. Lett.* **76**, 3251 (2000).
- <sup>5</sup>A. Polimeni, M. Bissiri, M. Felici, M. Capizzi, I. A. Buyanova, W. M. Chen, H. P. Xin, and C. W. Tu, *Phys. Rev. B* **67**, 201303 (2003).
- <sup>6</sup>I. A. Buyanova, G. Yu. Rudko, W. M. Chen, H. P. Xin, and C. W. Tu, *Appl. Phys. Lett.* **80**, 1740 (2002).
- <sup>7</sup>I. A. Buyanova, M. Izadifard, W. M. Chen, H. P. Xin, and C. W. Tu, *Phys. Rev. B* **69**, 201303 (2004).
- <sup>8</sup>M. Felici, A. Polimeni, M. Capizzi, S. V. Dudy, A. Zunger, I. A. Buyanova, M. W. Chen, H. P. Xin, and C. W. Tu (unpublished).
- <sup>9</sup>H. Yaguchi, S. Miyoshi, G. Biwa, M. Kibune, K. Onabe, Y. Shiraki, and R. Ito, *J. Cryst. Growth* **170**, 353 (1997).
- <sup>10</sup>C. V. Reddy, R. E. Martinez II, V. Narayanamurti, H. P. Xin, and C. W. Tu, *Phys. Rev. B* **66**, 235313 (2002).
- <sup>11</sup>S. Yoon, M. J. Seong, J. F. Geisz, A. Duda, and A. Mascarenhas, *Phys. Rev. B* **67**, 235209 (2003).
- <sup>12</sup>G. Leibiger, V. Gottschalch, M. Schubert, G. Benndorf, and R. Schwabe, *Phys. Rev. B* **65**, 245207 (2002).
- <sup>13</sup>H. Kanaya, H. Yaguchi, Y. Hijakata, S. Yoshida, S. Miyoshi, and K. Onabe, *Phys. Status Solidi C* **0**, 2753 (2003).
- <sup>14</sup>Y. Zhang, B. Fluegel, M. C. Hanna, J. F. Geisz, L.-W. Wang, and A. Mascarenhas, *Phys. Status Solidi B* **240**, 396 (2003).
- <sup>15</sup>P. R. C. Kent and A. Zunger, *Phys. Rev. Lett.* **86**, 2613 (2001); *Phys. Rev. B* **64**, 115208 (2001).
- <sup>16</sup>B. A. Weinstein, S. R. Stambach, T. M. Ritter, J. O. Maclean, and D. J. Wallis, *Phys. Rev. B* **68**, 035336 (2003).
- <sup>17</sup>P. N. Hai, W. M. Chen, I. A. Buyanova, B. Monemar, H. P. Xin, and C. W. Tu, *Mater. Sci. Eng., B* **82**, 218 (2001).
- <sup>18</sup>F. Masia, A. Polimeni, G. B. H. von Högersthal, M. Bissiri, M. Capizzi, P. J. Klar, and W. Stoltz, *Appl. Phys. Lett.* **82**, 4474 (2003).
- <sup>19</sup>Y. Zhang, A. Mascarenhas, H. P. Xin, and C. W. Tu, *Phys. Rev. B* **61**, 7479 (2000).
- <sup>20</sup>L. Bellaiche, S.-H. Wei, and A. Zunger, *Phys. Rev. B* **54**, 17 568 (1996); **56**, 10 233 (1997).
- <sup>21</sup>T. Mattila, L.-W. Wang, and A. Zunger, *Phys. Rev. B* **59**, 15 270 (1999).
- <sup>22</sup>P. Keating, *Phys. Rev.* **145**, 637 (1966).
- <sup>23</sup>K. A. Mader and A. Zunger, *Phys. Rev. B* **50**, 17 393 (1994).
- <sup>24</sup>L.-W. Wang, J. Kim, and A. Zunger, *Phys. Rev. B* **59**, 5678 (1999).
- <sup>25</sup>L.-W. Wang and A. Zunger, *J. Chem. Phys.* **100**, 2394 (1994).
- <sup>26</sup>L.-W. Wang, L. Bellaiche, S.-H. Wei, and A. Zunger, *Phys. Rev. Lett.* **80**, 4725 (1998).
- <sup>27</sup>T. N. Morgan, *Phys. Rev. Lett.* **21**, 819 (1968).